Journal of Hydroscience and Hydraulic Engineering
Vol. 3, No. 2, November, 1985, pp.15-30.

NUMERICAL CALCULATION OF POLLUTANT TRANSPORT IN ONE AND TWO DIMENSIONS

By

Toshimitsu Komatsu
Department of Civil Engineering Hydraulics and Soil Mechanics,
Kyushu University, Fukuoka 812, Japan

Forrest M. Holly Jr.
Department of Civil and Environmental Engineering,
The University of Iowa, Iowa City, IA 52242, USA

Norikazu Nakashiki
Department of Civil Engineering Hydraulics and Soil Mechanics,
Kyushu University, Fukuoka 812, Japan

and

Koichiro Ohgushi
Department of Civil Engineering Hydraulics and Soil Mechanics,
Kyushu University, Fukuoka 812, Japan

SYNOPSIS

The high accuracy of the two-point fourth-order Holly-Preissmann method for numerical calculation of contaminant advection is obtained by treating the spatial derivatives of concentration as dependent variables. In a split-operator approach for dispersion modelling, diffusion of both the concentration and its spatial derivatives must be computed, leading to a rather complicated algorithm in two dimensions. Holly-Komatsu proposed the eight-point method as an alternative approach which retains high accuracy but treats only the concentration as a dependent variable. However, there were some practical difficulties in two-dimensional implementation of the eight-point scheme. This paper describes the search for an improved approach which has almost the same accuracy but uses values of concentration only at six points. Some treatments of boundary condition in one and two dimensions are described in detail and their performance is demonstrated by application to schematic test cases. It is found that the six-point scheme performs well, being free of excessive numerical damping and oscillation.

INTRODUCTION

Mathematical modelling of the dispersion of passive contaminants in waterways and coastal zones involves the numerical solution of a partial differential equation which contains two kinds of transport; advection and diffusion. The diffusive transport can be computed accurately using a variety of finite difference and finite element numerical schemes. However, it has been more difficult to attain sufficient accuracy in numerical computation of advection.

The split-operator approach in which the advection and the diffusion are computed independently over short time increments has been pursued because of its advantage in allowing use of an accurate (but different) method for each process. In particular, this has made it possible to exploit the hyperbolic nature of advec-

tion to devise characteristics-based schemes which allow a natural treatment of boundary conditions and provide a framework for simple development of high accuracy methods.

Holly and Preissmann (2) proposed the two-point fourth-order method which computes advection with high accuracy but at the expense of carrying not only the concentration, but also its spatial derivatives, as dependent variables. These derivatives must themselves be both advected and diffused, which in a one-dimensional application is a straightforward , inexpensive procedure. However, in a two-dimensional application these additional computations become more complicated and expensive (Glass and Rodi (1), Holly and Usseglio-Polatera (4)).

Holly and Komatsu (3) reported the eight-point method as an alternative approach which retains high accuracy but treats only concentration as a dependent variable. However, there were some practical difficulties in more general implementation of the eight-point scheme as follows:

(1) Each interpolation in a two-dimensional case is based on 64 adjacent points, resulting in an overly cumbersome scheme.
(2) Concentration values at three points outside the boundary must be estimated, so that the accuracy of computational results may be compromised.
(3) Non-uniform grids may destroy symmetry-based accuracy.

In this paper, we propose an improved approach which has almost the same accuracy but uses values of concentration at only six points, and present some treatments of boundary conditions which are selected as the best compromise between accuracy and complexity. The six-point scheme is applied to one- and two-dimensional test cases. The numerical error associated with non-uniform computational grids or non-uniform flow fields is discussed in a one-dimensional case. The six-point method is applied to a river confluence as a one-dimensional practical case. In addition, the applications of this scheme to the pure advection of a concentration discontinuity and the dispersion of a Gaussian concentration distribution in a corner flow are demonstrated as examples of two-dimensional applications.

DERIVATION OF A SIX-POINT METHOD

Review of Characteristics-Based Computation of Advection

The characteristics approach is most easily explained in a one-dimensional context; its extension to multidimensions is immediate. The one-dimensional advection equation is written as:

$$\frac{\partial C}{\partial t} + U\frac{\partial C}{\partial x} = 0 \qquad (1)$$

with C(x,t)= concentration of contaminant; x=space coordinate; t=time; U(x,t)=water velocity. The left side of Eq. 1 is recognized as a total derivative, so it can be written as:

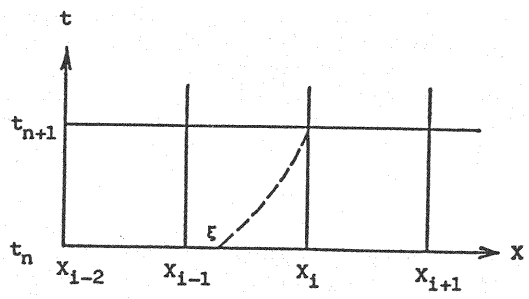

Fig. 1 Finite Difference Grid in One Space Dimension

$$\frac{dC}{dt} = 0 \qquad \text{along} \qquad \frac{dx}{dt} = U \qquad (2)$$

These ordinary differential equations state simply that the concentration must be constant along the space-time trajectory defined by U(x,t). Implementation of Eq. 2 in a mathematical model on the fixed Eulerian space-time grid of Fig. 1 implies that if the concentrations are known at all grid points at time level t_n, the unknown concentration at any point at time level t_{n+1} is obtained from the solution to Eq. 2:

$$C_i^{n+1} = C_\xi^n \qquad (3)$$

where superscript n denotes time level t_n, subscript i denotes computational point x_i, and ξ denotes the x-coordinate of the foot of the trajectory leading to the point (x_i, t_{n+1}). The problem of the finding the "new" concentration at point x_i at time t_{n+1} reduces to the problem of knowing the "old" concentration at ξ at time t_n. For that reason the accuracy of scheme is dependent on how accurately we estimate C^n_ξ.

The Six-Point Method

Fig. 2 shows a one-dimensional grid in an interior region, with no boundary influence.

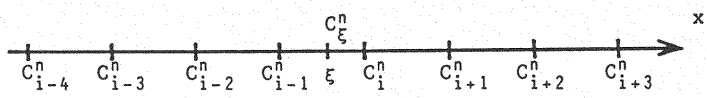

Fig. 2 One-Dimensional Computational Grid in an Interior Region

Expansions of C around x_{i-1} in a Taylor series result in expressions for C_{i-2}, C_{i-3} and C_{i-4} as follows:

$$C_{i-2} = C_{i-1} - CX_{i-1}(\Delta x) + \frac{1}{2!}CXX_{i-1}(\Delta x)^2 - \frac{1}{3!}CXXX_{i-1}(\Delta x)^3 + \cdots$$

$$C_{i-3} = C_{i-1} - CX_{i-1}(2\Delta x) + \frac{1}{2!}CXX_{i-1}(2\Delta x)^2 - \frac{1}{3!}CXXX_{i-1}(2\Delta x)^3 + \cdots \quad (4)$$

$$C_{i-4} = C_{i-1} - CX_{i-1}(3\Delta x) + \frac{1}{2!}CXX_{i-1}(3\Delta x)^2 - \frac{1}{3!}CXXX_{i-1}(3\Delta x)^3 + \cdots$$

where Δx = grid spacing; $CXX = \partial^2 C/\partial x^2$ and $CXXX = \partial^3 C/\partial x^3$. If terms in Eq. 4 of order three or higher are neglected, three variables, that is, CX_{i-1}, CXX_{i-1}, $CXXX_{i-1}$, are left as unknowns. We can determine CX_{i-1}, by solving Eq. 4 as a set of simultaneous equations.

Using concentrations at the seven points from x_{i-4} to x_{i+2}, four combinations of the Taylor series expansions can be similarly constructed on successive four-point sequences, i.e. (i-4 to i-1; i-3 to i; ...; i-1 to i+2). These combinations are denoted by superscripts (1) to (4) and solved to obtain derivative estimates at point x_{i-1}:

$$\begin{aligned} CX^{(1)}_{i-1} &= f(C^n_{i-4}, C^n_{i-3}, C^n_{i-2}, C^n_{i-1}) \\ CX^{(2)}_{i-1} &= f(C^n_{i-3}, C^n_{i-2}, C^n_{i-1}, C^n_i) \end{aligned} \quad (5)$$

and similarly for $CX^{(3)}_{i-1}$, $CX^{(4)}_{i-1}$.

Denoting by superscripts (2) to (5) other combinations of the Taylor series expansions around x_i in the same way, derivative estimates at point x_i are written as follows:

$$\begin{aligned} CX^{(2)}_i &= f(C^n_{i-3}, C^n_{i-2}, C^n_{i-1}, C^n_i) \\ CX^{(3)}_i &= f(C^n_{i-2}, C^n_{i-1}, C^n_i, C^n_{i+1}) \\ &\vdots \\ CX^{(5)}_i &= f(C^n_i, C^n_{i+1}, C^n_{i+2}, C^n_{i+3}) \end{aligned} \quad (6)$$

Final estimates of CX^n_i and CX^n_{i-1} are obtained as weighted averages of four

series-expansion-derived values,

$$CX_{i-1}^n = \frac{1}{2(l+1)}\{CX_{i-1}^{(1)} + l\cdot CX_{i-1}^{(2)} + l\cdot CX_{i-1}^{(3)} + CX_{i-1}^{(4)}\}$$
$$CX_i^n = \frac{1}{2(l+1)}\{CX_i^{(2)} + l\cdot CX_i^{(3)} + l\cdot CX_i^{(4)} + CX_i^{(5)}\} \quad (7)$$

Use of these derivative estimates with C_i^n and C_{i-1}^n in the original compact method of Holly-Preissmann resulted in even less amplitude error, but generated more phase error as seen in spatial oscillation and negative concentrations. Through experimentation and intuitive reasoning it became apparent that the key to reducing the phase error would lie, not in attempting to generate higher derivatives, but in exploiting the known accuracy of CX estimates by generating an estimate of $CX_{i-\frac{1}{2}}^n$, then averaging two compact polynomials to obtain C_ξ^n. Three of the five combinations of series-expansions were adopted to estimate $CX_{i-\frac{1}{2}}^n$ at $x_{i-\frac{1}{2}}$, then averaged to obtain:

$$CX_{i-\frac{1}{2}}^n = \frac{1}{m+2}\{CX_{i-\frac{1}{2}}^{(2)} + m\cdot CX_{i-\frac{1}{2}}^{(3)} + CX_{i-\frac{1}{2}}^{(4)}\} \quad (8)$$

Optimum values for the weights l and m will be discussed later.

The final determination of C_ξ^n used a direct averaging of two compact cubic polynomials, one constructed using C_{i-1}^n, CX_{i-1}^n, $CX_{i-\frac{1}{2}}^n$ and C_i^n, the other using C_{i-1}^n, $CX_{i-\frac{1}{2}}^n$, CX_i^n and C_i^n.

$$C_i^{n+1} = A_1C_{i-4}^n + A_2C_{i-3}^n + A_3C_{i-2}^n + A_4C_{i-1}^n + A_5C_i^n + A_6C_{i+1}^n + A_7C_{i+2}^n + A_8C_{i+3}^n \quad (9)$$

with $A_1, \ldots, A_8$ = cubic polynomials in α, involving weights l and m, where $\alpha = (x_i - \xi)/(x_i - x_{i-1})$.

Eq. 9 is constructed using the eight C-values and is almost the same as the eight-point method. The final goal of this study is to develop a more compact method than the eight-point method. To do this, we must decrease the number of C-values used in Eq. 9. C_{i-4}^n and C_{i+3}^n at both ends appear in $CX_{i-1}^{(1)}$, $CX_i^{(5)}$ respectively. Detailed analysis of Eq. 9 showed that $CX_{i-1}^{(1)}$ and $CX_i^{(5)}$ in Eq. 7 played important roles in cancelling errors which were included in $CX_{i-1}^{(4)}$ and $CX_i^{(2)}$ respectively. Therefore it should be avoided to drop $CX_{i-1}^{(1)}$, $CX_i^{(5)}$ in estimating CX_{i-1}, CX_i in order to decrease the number of C-values. Simple linear extrapolations are adopted to estimate C_{i-4} and C_{i+3}.

$$C'_{i-4} = 2C_{i-3} - C_{i-2}$$
$$C'_{i+3} = 2C_{i+2} - C_{i+1} \quad (10)$$

where C'_{i-4} and C'_{i+3} are the estimated values of C_{i-4} and C_{i+3} respectively. Assuming $C_{i-4} = C'_{i-4}$, $C_{i+3} = C'_{i+3}$ and rearranging Eq. 9 by substituting Eq. 10 into Eqs. 5 and 6, the following six-point method results:

$$C_i^{n+1} = \sum_{k=1}^{6} b_k \cdot C_{i+k-4}^n \quad (11)$$

with $b_k (k = 1, \ldots, 6)$ = cubic polynomials in α.

The Taylor-series analysis of Eq. 11 reveals that the leading term of the truncation error is the second one because of the linear extrapolations in Eq. 10, i.e.

$$\frac{\partial C}{\partial t} + U\frac{\partial C}{\partial x} = \{-\beta_1\alpha^2 + \beta_1\alpha\}\frac{\partial^2 C}{\partial x^2}\frac{(\Delta x)^2}{2!} + \{\beta_2\alpha^2 - \beta_2\alpha\}\frac{\partial^3 C}{\partial x^3}\frac{(\Delta x)^3}{3!}$$

$$+ [-\alpha^4 + 2\alpha^3 + \{-3 + \beta_3\}\alpha^2 + \{2 - \beta_3\}\alpha]\frac{\partial^4 C}{\partial x^4}\frac{(\Delta x)^4}{4!}$$

$$+ [\alpha^5 - 5r_1\alpha^3 + \{\frac{15}{2}r_1 - \beta_4\}\alpha^2 + \{-r_2 + \beta_4\}\alpha]\frac{\partial^5 C}{\partial x^5}\frac{(\Delta x)^5}{5!} + \cdots \qquad (12)$$

with

$$\beta_1 = \frac{1}{3(l+1)}\ ,\ \beta_2 = \frac{1}{2(l+1)}\ ,\ \beta_3 = \frac{6l-34}{3(l+1)}\ ,\ \beta_4 = \frac{5(l-12)}{2(l+1)}\ ,\ r_1 = \frac{m+6}{m+2}\ ,\ r_2 = \frac{7m+34}{2(m+2)}$$

when u and Δx are constant. We evaluated the value of m so as to minimize the artificial dispersion coefficient of the fifth order term by using the method of least squares, i.e.,

$$\int_0^1 \{5\text{th order a.d.c.}\}^2 d\alpha = \text{minimum},$$

yielding:

$$m = -11.23 \qquad (13)$$

where a.d.c. is an abbreviation of "artificial dispersion coefficient". The second, third and fourth order artificial dispersion coefficients all include the weight l. Since there is no unique solution which makes each of the squares of the second, third and fourth a.d.c. minimum at the same time, l cannot be determined theoretically. Experimental results suggest that $l = 9.55$ gives the best computational results for the Gaussian model problem.

The above detailed procedures, whose descriptions serve to illustrate the reasoning behind the method, can be forgotten when implementing the final algebraic expression which incorpolates them:

$$C_i^{n+1} = b_1 C_{i-3}^n + b_2 C_{i-2}^n + b_3 C_{i-1}^n + b_4 C_i^n + b_5 C_{i+1}^n + b_6 C_{i+2}^n \qquad (14)$$

with

$$b_1 = -0.01806\alpha^3 - 0.03828\alpha^2 + 0.05633\alpha$$

$$b_2 = 0.2570\alpha^3 + 0.05276\alpha^2 - 0.3097\alpha$$

$$b_3 = -0.6806\alpha^3 + 0.6480\alpha^2 + 1.033\alpha$$

$$b_4 = 0.6806\alpha^3 - 1.394\alpha^2 - 0.2869\alpha + 1$$

$$b_5 = -0.2570\alpha^3 + 0.8236\alpha^2 - 0.5667\alpha$$

$$b_6 = 0.01806\alpha^3 - 0.09245\alpha^2 + 0.07439\alpha$$

Demonstration and Evaluation of Method

One-Dimensional Case

The pure advection of a Gaussian concentration distribution in an infinitely long channel of unit width and constant velocity 0.5m/s is the situation used here to demonstrate the six-point scheme. The Gaussian distribution of standard deviation 264m is defined on a regular grid of Δx = 200m. This initial distribution is

transported downstream for 9,600s. Fig. 3 shows the exact solution and computed ones with Δt = 100s using the six-point scheme (Eq. 14), the eight-point scheme, Holly-Preissmann scheme and the first-order explicit upwind difference scheme derived from Eq. 1. Using the same four methods and the same situation, Fig. 4 shows the computed advection of a trapezoidal distribution.

It is clear that the last scheme introduces an excessive artificial diffusion. The six-point scheme retains almost the same accuracy as the eight-point method and the Holly-Preissmann scheme, and its execution is much simpler for a two-dimensional case, particularly when it is compared with the Holly-Preissmann scheme as we will show in the following section.

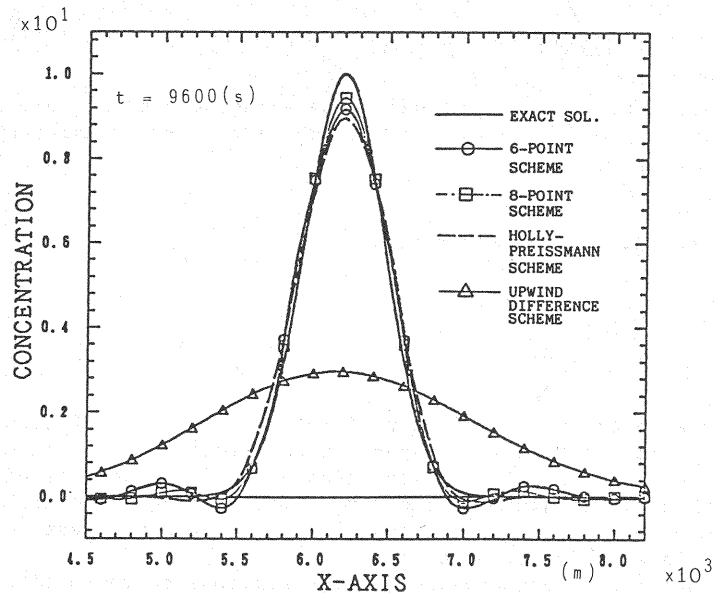

Fig. 3 Comparison of Exact and Numerical Solutions

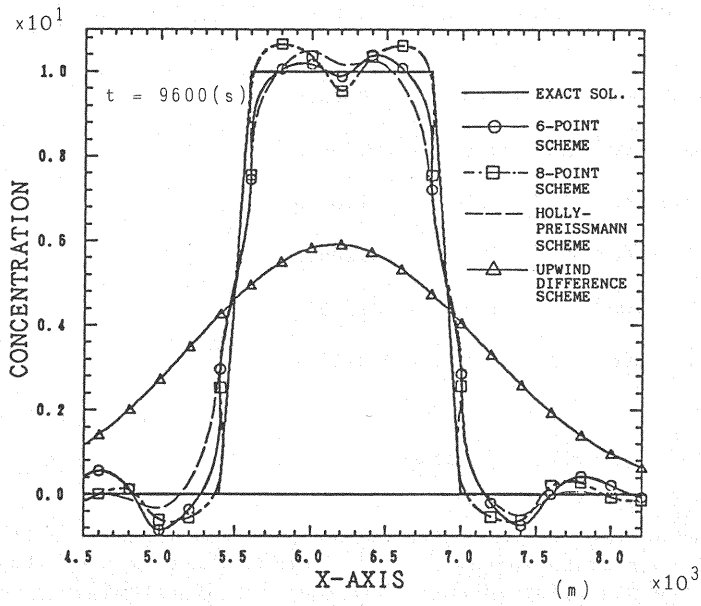

Fig. 4 Comparison of Exact and Numerical Solutions

The Extension of the Method to Two-Dimensional Problems

Application of the six-point method to two dimensions is straightforward. Eq. 2 becomes:

$$\frac{dC}{dt} = 0 \qquad \text{along} \qquad \frac{dx}{dt} = U \ , \ \frac{dy}{dt} = V \tag{15}$$

where V(x,y,t) is the y-direction velocity, and now C = C(x,y,t) and U = U(x,y,t). The solution is

$$C_{i,j}^{n+1} = C_{\xi,\eta}^{n} \tag{16}$$

where as shown in Fig. 5, j is the y-direction index of grid points, and (ξ,η) are the x-y coordinates of the intersection of the trajectory with the x-y plane at time of t_n. The interpolating polynomial for $C_{\xi,\eta}^{n}$ is constructed by successive use of Eq. 14 along six grid lines in one direction, and one final use in the perpendicular direction. Formally the resulting scheme can be written

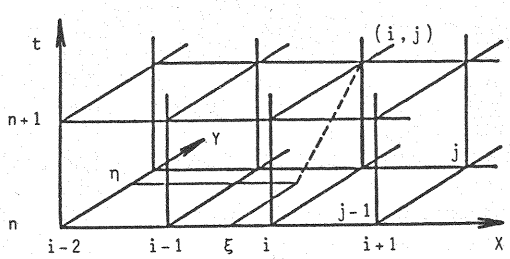

Fig. 5 Finite Difference Grid in Two Space Dimensions

$$C_{i,j}^{n+1} = \sum_{p=1}^{6} \sum_{s=1}^{6} b_{ps} C_{i+p-4,\,j+s-4}^{n} \tag{17}$$

i.e. it involves concentrations at 36 surrounding grid points.

The steady velocity field shown on Fig. 6 represents a rigid-body rotation at an angular velocity of 2π radians in 12,000s. At the time t = 0s four Gaussian distributions of $\sigma_x = \sigma_y = 200$m are placed in each quadrant. Fig. 7 shows the results produced by the characteristics advection calculation after a quarter tour using $\Delta t = 100$s, $\Delta x = \Delta y = 100$m with the two-dimensional Holly-Preissmann result (Holly, Usseglio-Polatera (4)) and the eight-point method's result shown for comparison. While Holly-Preissmann's error in peak concentration is 1.8%, the six-point method's one is 1.1%. In case of the eight-point method, the error is 0.5%.

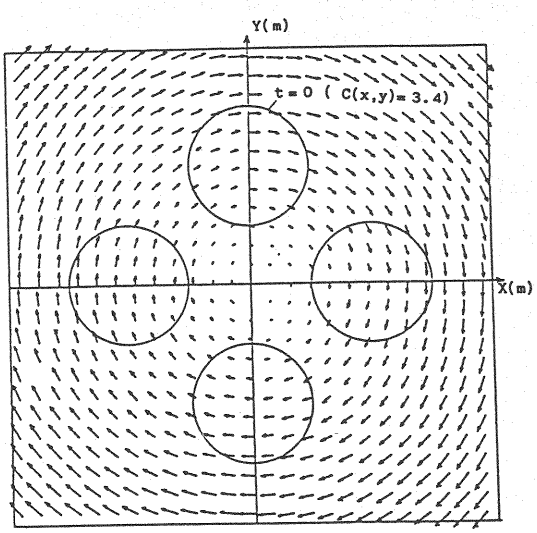

Fig. 6 Calculations of Two-Dimensional Circular Advection

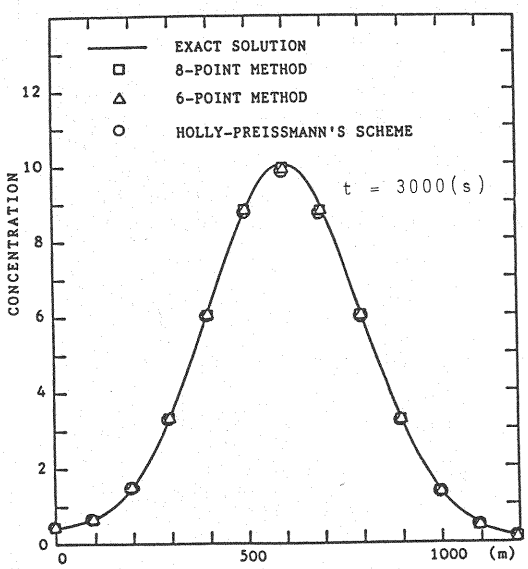

Fig. 7 Comparison of Exact and Numerical Solutions

BOUNDARY CONDITIONS IN ONE- AND TWO-DIMENSIONS

It was shown earlier that the six-point method was very useful in flow fields where the boundary conditions were of no importance. In most practical situations, however, the boundary conditions have direct effects upon the pollutant transport. Some considerations are needed at the boundary to put the six-point scheme to use. Therefore, we shall now discuss how to deal with the boundary conditions. Many trials were discussed and examined, and the one described in detail in the sequel was selected as the best compromise between accuracy and complexity.

One-Dimensional Case

Two types of computational domains are sketched in Figs. 8(a) and 8(b). In Fig. 8(a), every chracteristic enters through the boundary of the solution domain and one boundary condition on concentration must be given. On the other hand, at the boundary shown in Fig. 8(b) the characteristic goes out and no boundary condition is needed. In any case, application of the six-point scheme to the boundary requires that two artificial points be created outside the boundary. A pure advection equation is adopted at the boundary to relate the time and spatial derivatives.

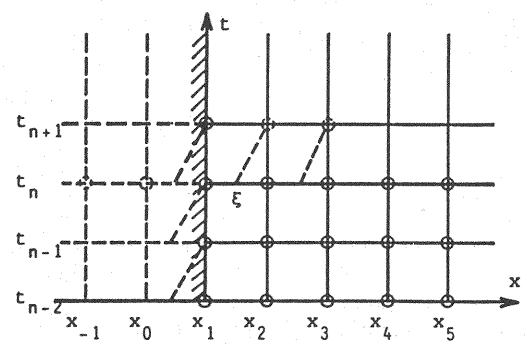

Fig. 8(a) The Boundary Which Every Characteristic Enters through

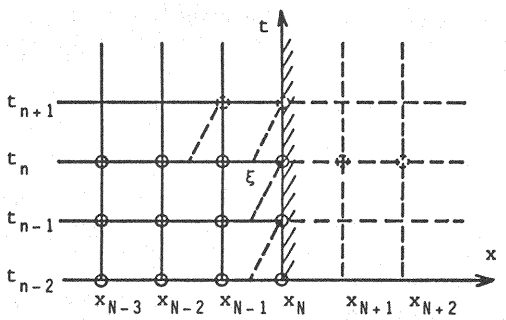

Fig. 8(b) The Boundary Which Every Characteristic Goes out of

We first consider the case shown in Fig. 8(a) when the boundary condition is given. Since we use values C^n_{-1}, C^n_0 to calculate C^{n+1}_2 with the six-point scheme, it is necessary to estimate them somehow. Expanding C^n around x_1 in the Taylor series, C^n_{-1} and C^n_0 are expressed by:

$$\begin{aligned} C^n_{-1} &= C^n_1 - 2\,CX^n_1\Delta x + 2\,CXX^n_1\Delta x^2 + \cdots \\ C^n_0 &= C^n_1 - CX^n_1\Delta x + \frac{1}{2}CXX^n_1\Delta x^2 + \cdots \end{aligned} \tag{18}$$

Assuming that the pure advection equation holds at the boundary to a good approximation, the following equation is obtained:

$$\left.\frac{\partial C}{\partial t}\right|_{x_1} + U(x_1,t)\left.\frac{\partial C}{\partial x}\right|_{x_1} = 0 \tag{19}$$

which results in

$$\begin{aligned} \left.\frac{\partial C}{\partial x}\right|_{x_1,t_n} &= \frac{-1}{U(x_1,\,t_n)}\left.\frac{\partial C}{\partial t}\right|_{x_1,t_n} \\ \left.\frac{\partial^2 C}{\partial x^2}\right|_{x_1,t_n} &= \frac{1}{(U(x_1,\,t_n))^2}\left.\frac{\partial^2 C}{\partial t^2}\right|_{x_1,t_n} + \frac{1}{(U(x_1,\,t_n))^2}\left.\frac{\partial U}{\partial t}\right|_{x_1,t_n}\cdot\left.\frac{\partial C}{\partial x}\right|_{x_1,t_n} \\ &\quad - \frac{1}{U(x_1,\,t_n)}\left.\frac{\partial U}{\partial x}\right|_{x_1,t_n}\cdot\left.\frac{\partial C}{\partial x}\right|_{x_1,t_n} \end{aligned} \tag{20}$$

where $\partial U/\partial t|_{x_1,t_n}$, $\partial U/\partial x|_{x_1,t_n}$ are known quantities, as the flow properties are given. For simplicity, consider the case when the velocity U(x,t) is constant at the boundary. Then Eq. 20 reduces to

$$CX_1^n = -\frac{1}{U}\frac{\partial C}{\partial t}\bigg|_{x_1,t_n}$$
$$CXX_1^n = \frac{1}{U^2}\frac{\partial^2 C}{\partial t^2}\bigg|_{x_1,t_n} \tag{21}$$

Expansions of C_1 around t_n in the Taylor series result in the expressions for C_1^{n-1} and C_1^{n-2} as follows:

$$C_1^{n-1} = C_1^n - \frac{\partial C}{\partial t}\bigg|_{x_1,t_n}\Delta t + \frac{1}{2}\frac{\partial^2 C}{\partial t^2}\bigg|_{x_1,t_n}\Delta t^2 + \ldots$$
$$C_1^{n-2} = C_1^n - 2\cdot\frac{\partial C}{\partial t}\bigg|_{x_1,t_n}\Delta t + 2\cdot\frac{\partial^2 C}{\partial t^2}\bigg|_{x_1,t_n}\Delta t^2 + \ldots \tag{22}$$

If higher order terms than the second order in Eq. 22 are neglected, two variables, that is, $\partial C/\partial t|_{x_1,t_n}$, $\partial^2 C/\partial t^2|_{x_1,t_n}$ are left as unknowns. We can determine these variables by solving Eq. 22 as a set of simultaneous equations:

$$\frac{\partial C}{\partial t}\bigg|_{x_1,t_n} = \frac{1}{2\Delta t}(C_1^{n-2} - 4C_1^{n-1} + 3C_1^n)$$
$$\frac{\partial^2 C}{\partial t^2}\bigg|_{x_1,t_n} = \frac{1}{\Delta t^2}(C_1^{n-2} - 2C_1^{n-1} + C_1^n) \tag{23}$$

Substituting the results obtained by eliminating $\partial C/\partial t$ and $\partial^2 C/\partial t^2$ from Eqs. 21 and 23 into Eq. 18, we obtain:

$$C_{-1}^n = \frac{\alpha+2}{\alpha^2}C_1^{n-2} - \frac{4(\alpha+1)}{\alpha^2}C_1^{n-1} + \frac{(\alpha+1)(\alpha+2)}{\alpha^2}C_1^n$$
$$C_0^n = \frac{\alpha+1}{2\alpha^2}C_1^{n-2} - \frac{2\alpha+1}{\alpha^2}C_1^{n-1} + \frac{(2\alpha+1)(\alpha+1)}{2\alpha^2}C_1^n \tag{24}$$

Thus the values of C_{-1}^n and C_0^n can be estimated, as C_1^{n-2}, C_1^{n-1} and C_1^n are all known.

The two values C_{N+1}^n, C_{N+2}^n at the artificial points in Fig. 8(b) are estimated in the same way; the final expressions are:

$$C_{N+1}^n = \frac{-(\alpha-1)}{2\alpha^2}C_N^{n-2} + \frac{2\alpha-1}{\alpha^2}C_N^{n-1} + \frac{(2\alpha-1)(\alpha-1)}{2\alpha^2}C_N^n$$
$$C_{N+2}^n = \frac{-(\alpha-2)}{\alpha^2}C_N^{n-2} + \frac{4(\alpha-1)}{\alpha^2}C_N^{n-1} + \frac{(\alpha-1)(\alpha-2)}{\alpha^2}C_N^n \tag{25}$$

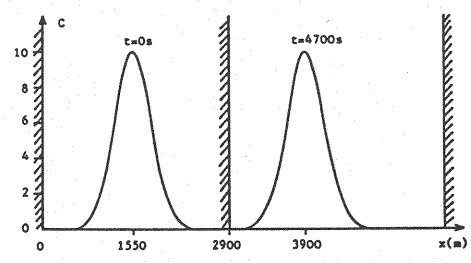

Fig. 9 Calculations of One-Dimensional Advection Using Two Treatments of Boundary Condition

When the velocities $U(x_1,t)$, $U(x_N,t)$ at the boundaries are not constant, we must use Eq. 20 instead of Eq. 21. In order to inspect the validity of Eqs. 24 and 25, the advection of a Gaussian concentration distribution is computed in two ways as is shown in Fig. 9. The flow conditions are the same as those described earlier.

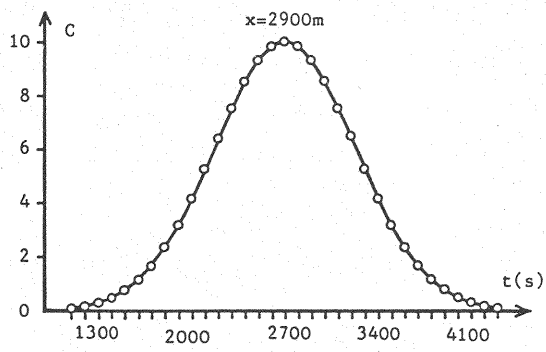

Fig. 10 The Boundary Condition Given When the Boundary is Situated at x=2,900m

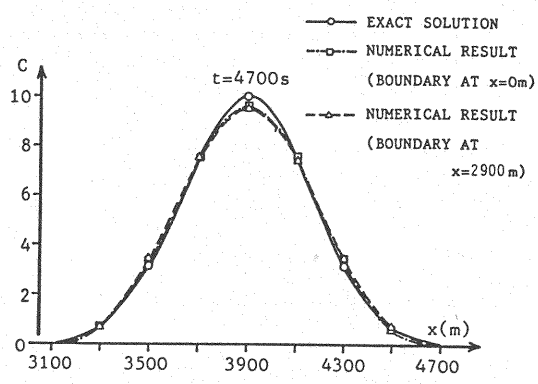

Fig. 11 Influence of Errors in Treatments of Boundary Condition

First, in case the upstream boundary of domain is situated at x = 0m, the treatment of boundary conditions has little effect on the computational results. Alternatively, when the boundary condition which corresponds to the previous case is given at x = 2,900m by the time-dependent concentration shown in Fig. 10, the accuracy of computation depends strongly on that of Eq. 24. Fig. 11 shows the results of both cases at t = 4,700s and the exact solution. There is a little damping in the computational results compared with the exact solution, but no remarkable difference between the two cases is evident. It means that Eqs. 24 and 25 are valid in estimating the concentration values outside the boundary.

Though the use of Eq. 24 or Eq. 25 requires the concentration values at a few time step before the initial condition, we can assume them to be equal to the initial condition. It is expected that the inconsistensies introduced by this assumption will have minor influence on the results.

Two-Dimensional Case

The boundary of a two-dimensional computation domain is shown in Fig. 12. On applying the six-point method to the boundary in two dimensions, it is also necessary to create two artificial points outside the boundary. Using a Taylor series development, we can find the values of $C^n_{i-2,j}$, $C^n_{i-1,j}$:

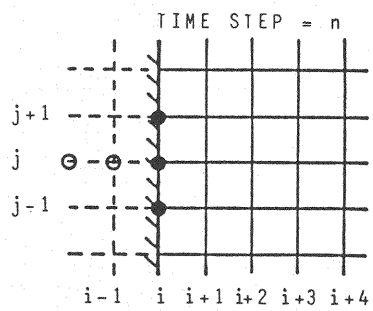

Fig. 12 Finite Difference Grid in Two Space Dimensions

$$C^n_{i-2,j} = C^n_{i,j} - 2\Delta x \left.\frac{\partial C}{\partial x}\right|_{i,j,n} + \cdots$$

$$C^n_{i-1,j} = C^n_{i,j} - \Delta x \left.\frac{\partial C}{\partial x}\right|_{i,j,n} + \cdots \qquad (26)$$

Assuming again here that the pure-advection equation holds approximately at the boundary, the following equation is given:

$$\left.\frac{\partial C}{\partial t}\right|_{i,j,n} + U(x_i, y_j, t_n)\left.\frac{\partial C}{\partial x}\right|_{i,j,n} + V(x_i, y_j, t_n)\left.\frac{\partial C}{\partial y}\right|_{i,j,n} = 0 \qquad (27)$$

Expanding $C_{i,j}$ around $t = t_n$ in the Taylor series, we obtain expressions for $C^{n-1}_{i,j}$, $C^{n-2}_{i,j}$, in which terms higher than the second order are neglected. We can determine $\partial C/\partial t|_{i,j,n}$, $\partial^2 C/\partial t^2|_{i,j,n}$ solving the expressions for $C^{n-1}_{i,j}$ and $C^{n-2}_{i,j}$ as a set of simultaneous equations. As a result,

$$\left.\frac{\partial C}{\partial t}\right|_{i,j,n} = \frac{1}{2\Delta t}(3C^n_{i,j} - 4C^{n-1}_{i,j} + C^{n-2}_{i,j}) \tag{28}$$

is given. Then, we adopt a central difference to discretize $\partial C/\partial y|_{i,j,n}$:

$$\left.\frac{\partial C}{\partial y}\right|_{i,j,n} = \frac{1}{2\Delta y}(C^n_{i,j+1} - C^n_{i,j-1}) \tag{29}$$

By substituting Eqs. 28 and 29 into Eq. 27 and then substituting the result into Eq. 26, the following equations are given as expressions for estimating the concentrations outside the boundary:

$$\begin{aligned} C^n_{i-2,j} &= \frac{\Delta x}{U}\left[\frac{1}{\Delta t}(3C^n_{i,j} - 4C^{n-1}_{i,j} + C^{n-2}_{i,j}) + \frac{V}{\Delta y}(C^n_{i,j+1} - C^n_{i,j-1})\right] + C^n_{i,j} \\ C^n_{i-1,j} &= \frac{\Delta x}{2U}\left[\frac{1}{\Delta t}(3C^n_{i,j} - 4C^{n-1}_{i,j} + C^{n-2}_{i,j}) + \frac{V}{\Delta y}(C^n_{i,j+1} - C^n_{i,j-1})\right] + C^n_{i,j} \end{aligned} \tag{30}$$

When the boundary of the computational domain is situated along the x-axis, a similar treatment can be given.

In order to examine the validity of Eq. 30, we now apply the six-point scheme to a model problem of two-dimensional pure advection in which the treatment of boundary conditions is important. The steady velocity field shown on Fig. 13 represents rigid-body rotation at an angular velocity of 2π radians in 12,000s. At time t = 0s four Gaussian distributions of $\sigma_x = \sigma_y = 200$m are placed on each axis at distances ±600m far from the origin. As the computational domain is restricted to a square of which the side is 1,400m long, the boundary conditions have significant values as shown on Fig. 14. The mesh size is a uniform $\Delta x = \Delta y = 100$m and the time step is $\Delta t = 100$s. In this flow the Gaussian should undergo no deformation due to advection. Fig. 14 shows the concentration distribution after 1/4-turn of rotation using the six-point scheme and Eq. 30. The obtained result is consistent with the initial distribution and the error in peak concentration is 1.0%. Therefore, Eq. 30 would appear to be valid.

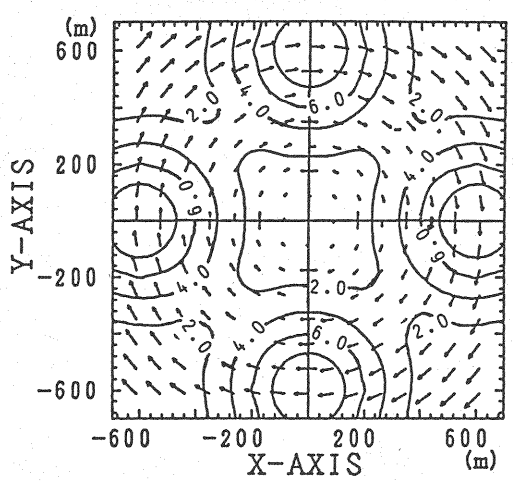

Fig. 13 Steady Velocity Field with a Two-Dimensional Circular Advection

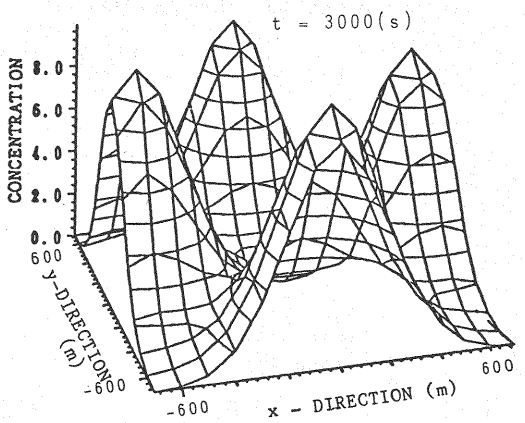

Fig. 14 Computed Result after after 1/4-turn of Rotation

EXTENSIONS OF SIX-POINT METHOD

Non-Constant Velocity

Let us consider the effects of non-constant velocity and non-uniform computational grid on the calculated results. First, suppose the non-constant velocity flow field shown in Fig. 15 where the velocity is 1.0m/s in the region of x = 3,200 - 4,400m and 0.5m/s in the other regions. The initial condition and the computational grid are the same as those described earlier. On applying the six-point scheme to a non-constant velocity flow, the α-value ($=U(x,t)\cdot\Delta t/\Delta x$) is variable and depends on the velocity. The result obtained at t = 7,200s is shown in Fig. 16 with the constant-velocity result (U = 0.5m/s, t = 7,200s) for comparison. No significant distortion of curves is apparent in Fig. 16.

Non-Uniform Computational Grid

In practical situations, a variable computational mesh is routinely used to save computer time and cost. Since the six-point scheme is formulated on the basis of a uniform grid, some of its accuracy will be lost when it is applied to a variable grid. However, it is expected that this scheme should perform fairly well even on a non-uniform grid, as long as grid-size variations are not too abrupt.

Consider the computational domain where the grid distance is 100m in the region of x = 3,200 - 4,400m, and 200m in the other regions. The velocity is constant throughout the flow field, U = 0.5m/s and the other conditions are the same as those in the previous section. The computed result is coincidentally the same as the previous one shown in Fig. 16 because of the same variation of α. In Fig. 16, each x-coordinate is shifted so that each peak of computed concentration occupies the same point for comparison. It would appear that the six-point scheme is useful even on a non-uniform computational mesh.

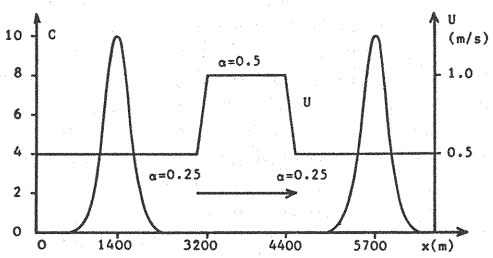

Fig. 15 Calculation of One-Dimensional Advection through Zone of Non-Constant Velocity

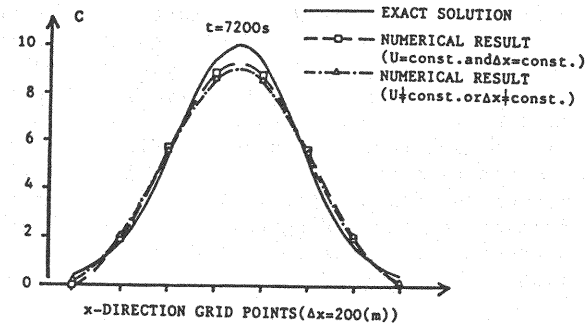

Fig. 16 Effect of Non-Constant Velocity or Non-Uniform Computational Grid

The River Confluence

The confluence and branching of a river are important and practical problems of one-dimensional pollutant transport. We now consider the application of the six-point scheme to a river confluence. Suppose that the river (1) with the cross-section S_1; velocity U_1; diffusivity D_1 and the river (2) with S_2; U_2; D_2 meet to start the river(3) with S_3; U_3; D_3 as shown in Figs. 17 and 18. The boundary conditions of concentration are given at the upstream boundaries of the rivers (1) and (2), so that the six-point scheme is easily applied to the rivers(1) and (2) using Eqs. 24 and 25. As for the river (3), a boundary condition of concentration at the confluence M must be generated. From the conservation of concentration flux at M, the following equation is obtained.

$$\{U_1S_1C_1(M) - S_1D_1(\frac{\partial C_1}{\partial x_1})_M\} + \{U_2S_2C_2(M) - S_2D_2(\frac{\partial C_2}{\partial x_2})_M\}$$

$$= \{U_3S_3C_3(M) - S_3D_3(\frac{\partial C_3}{\partial x_3})_M\} \qquad (31)$$

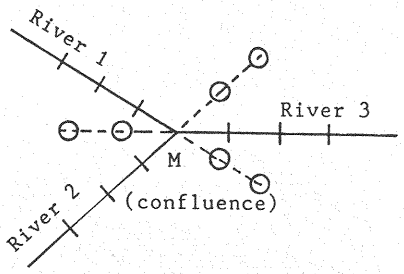

Fig. 17 One-Dimensional River Confluence

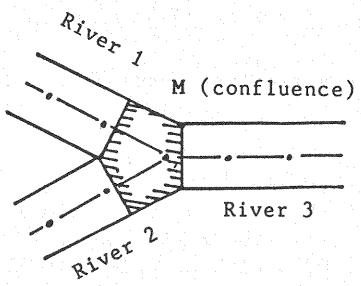

Fig. 18 Schematic Diagram of Confluence

in which $C_1(M)$ and $C_2(M)$ are the concentrations obtained at M from each computation of river (1) and (2).

Eq. 31 is discretized and only $dC/dx|_M$ is estimated by values at $t = t_{n-1}$, so that the estimated concentration $C_3(M)$ at $t = t_n$ for the river (3) is given by

$$C_3^n(M) = \frac{1}{U_3 S_3}\{U_1 S_1 C_1^n(M) + U_2 S_2 C_2^n(M) - S_1 D_1 \frac{C_1^n(M) - C_1^n(M-1)}{(\Delta x)_1} - S_2 D_2 \frac{C_2^n(M) - C_2^n(M-1)}{(\Delta x)_2} + S_3 D_3 \frac{C_3^{n-1}(M+1) - C_3^{n-1}(M)}{(\Delta x)_3}\} \quad (32)$$

Then, the six-point scheme can be easily applied to the river (3). The situation used here to show an example is given in Fig. 19, where $U_1 = 0.5$m/s, $U_2 = 1.0$m/s, $U_3 = 1.5$m/s, $D_1 = D_2 = D_3 = 3.78$m^2/s and the cross-section S_1, S_2, S_3 are constant. A Gaussian distribution with $\sigma = 264$m placed at a distance 2,000m apart from M in the river (1) and a trapezoidal one at a distance 6,000m apart from M in the river (2) are advected and diffused. The computed results successfully show this process in Figs. 20 and 21.

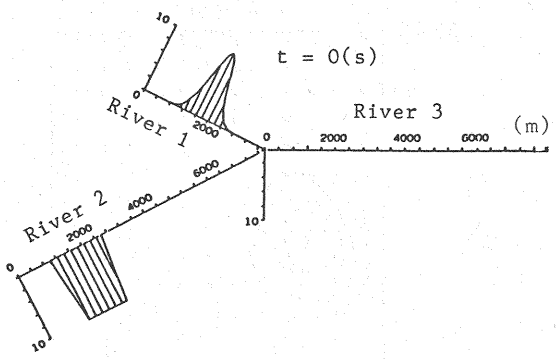

Fig. 19 Initial Concentration Distribution at t = 0 s

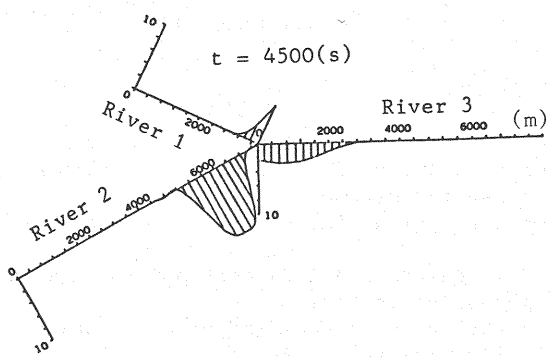

Fig. 20 Computed Concentration Distribution at t=4,500s

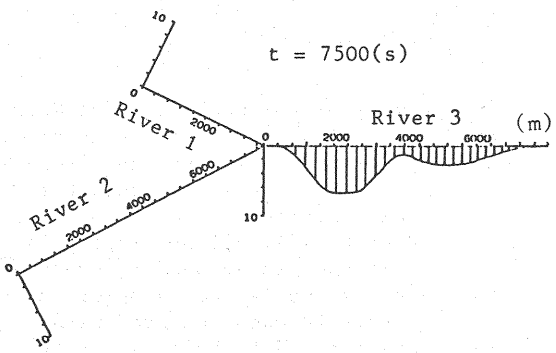

Fig. 21 Computed Concentration Distribution at t=7,500s

Pure Convection of Concentration Discontinuity

The six-point scheme is easily applied to two dimensions. We simulated the advection of a concentration discontinuity at a constant velocity aligned 45° to the Eulerian mesh (U = 0.5m/s, V = -0.5m/s). Fig. 22 shows the result computed at t = 3,000s with $\Delta x = \Delta y = 100$m, $\Delta t = 100$s. This scheme appears to reproduce a moving concentration discontinuity well.

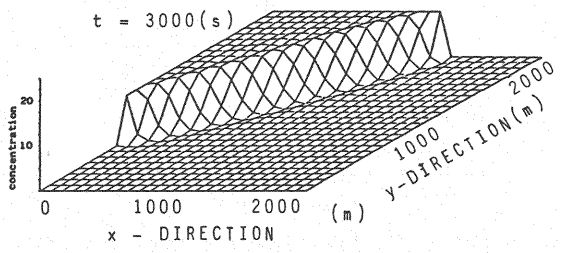

Fig. 22 Calculation of Advection of Concentration Discontinuity

Advection and Diffusion in a corner Flow

Lastly we simulate the advection and diffusion of a concentration distribution in a corner flow. A Gaussian distribution with $\sigma_x = \sigma_y = 264$m whose center is situated at x = -2,500m, y = 900m at t = 2,000s is advected and diffused in the flow field where U = -ax (m/s), V = ay (m/s) ($a = 3\times10^{-4}s^{-1}$) and the diffusivity $D = 20\sqrt{U^2+V^2}$ (m^2/s). Advection and diffusion are computed by the six-point scheme and the "Crank-Nicholson method", respectively. The boundary condition is treated by Eq. 30. The computed results in Figs. 23 and 24 show clearly that the Gaussian distribution is distorted in time by the advection and diffusion.

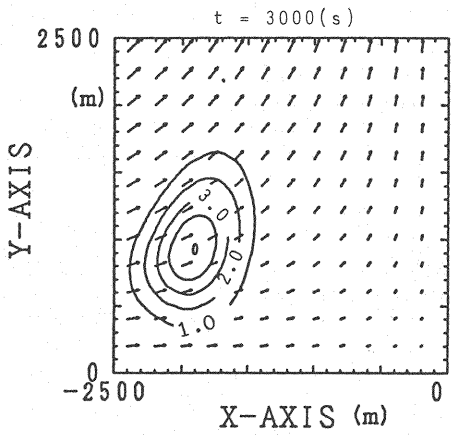

Fig. 23 Velocity Field at a Corner

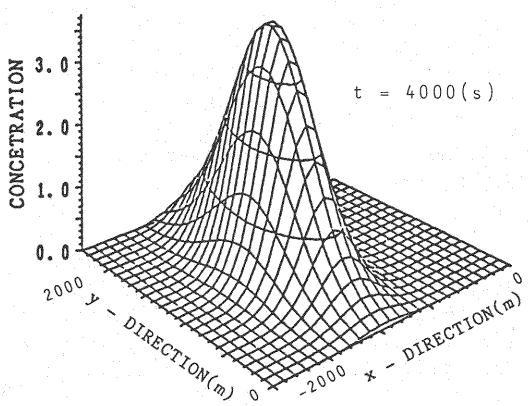

Fig. 24 Calculation of Advection and Diffusion of Gaussian Distribution

CONCLUSION

The six-point method has been developed on the basis of the eight-point method. Practical difficulties in the implementation of the eight-point scheme are reduced by dropping back to the accurate six-point method.

(1) The method retains almost the same accuracy as the eight-point method or Holly-Preissmann method.
(2) Each two-dimensional interpolation is based on 36 adjacent points, almost half the number needed for the eight-point method.
(3) The method is much simpler in computation for a two-dimensional case, particularly when compared with the Holly-Preissmann method.
(4) Practical difficulties for the treatment of boundary conditions are obviated by using Eq. 24 or Eq. 30.
(5) In the case of a non-uniform computational grid or non-constant velocity, there is no remarkable difference between the computed values and the exact

ones, which means that the six-point method is useful even under these conditions.

Based upon the results of this investigation, we have concluded that the six-point method is easily applied to various practical flow fields and very useful in calculation for advection not only in one-dimensional cases but also in two-dimensional ones.

Further exploration of the possible applications of the six-point method are presently in progress.

ACKNOWLEDGEMENT

The writers gratefully acknowledge the support provided by Iowa Institute of Hydraulic Research of the University of Iowa, Iowa City, Iowa, U.S.A. and Kyushu University. This work was supported by Japan Securities Scholarship Foundation.

REFERENCES

1. Glass, J. and W. Rodi : A higher order numerical scheme for scalar transport, Computer Method in Applied Mechanics and Engineering, Vol.31, pp.337-358, 1982.
2. Holly, F.M.Jr. and A. Preissmann : Accurate calculation of transport in two dimensions, JHYD, ASCE, Vol.103, No.HY11, pp.1259-1277, 1977.
3. Holly, F.M.Jr. and T. Komatsu : Derivative approximations in the two-point fourth-order method for pollutant transport, Proceedings of the Conference on Frontiers in Hydraulic Engineering, ASCE, Massachusetts Institute of Technology, Cambridge, U.S.A., pp.349-355, 1983.
4. Holly, F.M.Jr. and J.M. Usseglio-Polatera : Dispersion simulation in two-dimensional tidal flow, Journal of Hydraulic Engineering, ASCE, Vol.110, no.7, pp.905-926, 1984.
5. Morton, K.W. : Finite element methods for non-self-adjoint problems, Numerical Analysis Report 3/81, Dept. of Mathematics, Univ. of Reading, Reading, England, 1981.

APPENDIX - NOTATION

The following symbols are used in this paper:

a.d.c.	= artificial dispersion coefficient;
$A_1 - A_8$	= concentration interpolation coefficients in the 8-point scheme;
$b_1 - b_6$	= concentration interpolation coefficients in the 6-point scheme;
C(x,t), C(x,y,t)	= concentrations;
C'_{i-4}, C'_{i+3}	= estimated concentration values of C_{i-4}, C_{i+3} for the 6-point scheme;
CX(x,t)	= concentration derivative;
CXX(x,t)	= second concentration derivative;
CXXX(x,t)	= third concentration derivative;
D	= diffusivity;
$D_1 - D_3$	= diffusivities in rivers 1, 2 and 3 , respectively, in a river confluence;
i	= x-direction computational point index;
j	= y-direction computational point index;
l, m	= weight factors in estimation of CX;
M	= confluence point index;
n	= time index;

N	= total number of computational points;
r_1, r_2	= coefficients with respect to l in a.d.c.;
$S_1 - S_3$	= crose-sectional areas in rivers 1, 2 and 3, respectively, in a river confluence;
t	= time;
U	= x-direction water velocity;
V	= y-direction water velocity;
x, y	= orthogonal Cartesian distance coordinates;
α	= Courant number;
$\beta_1 - \beta_4$	= coefficients with respect to m in a.d.c.;
Δ	= prefix indicating incremental quantity;
η	= y-direction foot of the trajectory;
ξ	= x-direction foot of the trajectory; and
σ_x, σ_y	= standard deviations of a Gaussian distribution in x and y directions.